

Element abundance ratios in an extremely metal-poor binary star: CS 22873-139*

M. Spite¹, E. Depagne¹, B. Nordström², V. Hill³, R. Cayrel¹, F. Spite¹, and T.C. Beers⁴

¹ Observatoire de Paris-Meudon, DASGAL, URM 8633 du CNRS, 92125 Meudon Cedex, France
(Monique.Spite,Francois.Spite,Roger.Cayrel@obspm.fr)

² Niels Bohr Institute for Astronomy, Physics and Geophysics, Copenhagen University, Juliane Maries Vej 30, 2100 Copenhagen, Denmark
(birgitta@astro.ku.dk)

³ European Southern Observatory, Karl-Schwarzschild-Strasse 2, 85748 Garching bei München, Germany (vhill@eso.org)

⁴ Michigan State University, Department of Physics and Astronomy, East Lansing, MI 48824, USA (beers@pa.msu.edu)

Received 13 April 2000 / Accepted 13 June 2000

Abstract. High-resolution spectra of the extremely metal-poor double-lined spectroscopic binary star BPS CS 22873-139 have been analyzed to determine the metallicity and abundance ratios for a number of elements. From the analysis of the collected radial velocities, new orbital elements are derived as well as an improved mass ratio. In spite of its extreme metal deficiency, $[\text{Fe}/\text{H}] = -3.4$, the abundance ratios of CS 22873-139 are not similar to those of a typical Population II star. In particular, the α -elements are not enhanced relative to iron, and the strontium abundance is very low.

The abundance pattern of CS 22873-139 is compared to the patterns exhibited by other metal-poor stars which exhibit also very low strontium abundances. There is a large spread of elemental abundance ratios among these stars, suggesting that low strontium abundance may be associated with a variety of nucleosynthesis histories. The abundance ratios of CS 22873-139 are, surprisingly, very similar to those found in a common proper-motion pair HD 134439, HD 134440, even though the metallicity of this system is almost two dex higher, $[\text{Fe}/\text{H}] = -1.7$. The ratios are compared to those of another very metal-poor binary star BPS CS 22876-032. The unusual abundance pattern of CS 22873-139 is discussed (by comparison to the predicted yields of zero-metal SN II and hypernovae).

The lithium doublet at 6707 Å is not detected in CS 22873-139, but an abundance of lithium consistent with the Spite plateau cannot be excluded, based on the present data.

Key words: stars: abundances – stars: binaries: spectroscopic – stars: Population II – stars: individual: BPS CS 22873-139 – nuclear reactions, nucleosynthesis, abundances

1. Introduction

The star CS 22873-139 was identified as an extremely metal-poor candidate $[\text{Fe}/\text{H}] \approx -3.1$ in the HK objective-prism/interference-filter survey of Beers et al. (1985, 1992).

Send offprint requests to: M. Spite

* Based on observations made at the European Southern Observatory, La Silla, Chile

Its magnitude is $V = 13.83$ and its coordinates are

$$\alpha(2000) = 20^{\text{h}} 05^{\text{m}} 55.2^{\text{s}} \quad \delta(2000) = -59^{\circ} 17' 11''$$

Owing to its relatively bright apparent magnitude, CS 22873-139 is an attractive target for high-resolution observations in order to determine its elemental abundances, in spite of the difficulties introduced by its binarity.

Preston (1994) carried out an initial study of this star, obtaining a period estimate of 19.16 days, and a mass ratio of the two components $0.86 < M_{\text{B}}/M_{\text{A}} < 0.9$. Preston's model-dependent “decomposition” of CS 22873-139 led him to argue that the primary component might be classified as a “blue metal-poor main-sequence” star (BMP), as described in more detail by Preston et al. (1994). Furthermore, his comparison of the estimated luminosity ratios of the two components with the measured mass ratio suggested compatibility with an age of the system on the order of ~ 8 Gyr, which is surprisingly young for such a metal-deficient star. His conclusion was that this star may have been accreted from a low-luminosity satellite of the Milky Way sometime in the relatively recent past.

However, the spectroscopic data which Preston had available was of relatively low resolution ($R \sim 16,000$) and signal-to-noise ratio ($S/N \sim 25$), hence it was not feasible to derive accurate abundances for individual elements, and we sought to obtain data of the required quality, as examination of the relative elemental abundances might provide important clues to the origin of this star.

2. Observations and reductions

High-resolution spectroscopy of CS 22873-139 in the red portion of the spectrum (5000–8000 Å) was carried out with the ESO Multi-Mode Instrument (EMMI) at the 3.5-m New Technology Telescope (NTT), and in the blue (3900–5200 Å) with the CASPEC spectrograph at the 3.6m telescope at ESO, La Silla. The spectral resolving power, as measured from the FWHM of lines in the Th-Ar comparison spectra, is about $R = 50,000$ (FWHM ≈ 0.14 Å) for the EMMI spectra, and $R = 16,000$ for the CASPEC spectra (FWHM ≈ 0.28 Å). The

Table 1. Log of the observations

spectrum	date	exp. (min)	wavel. (Å)	S/N*
EMMI-971018	97-10-18	120	5000-8000	110
EMMI-971020	97-10-20	120	5000-8000	120
EMMI-990811	99-08-11	180	5000-8000	130
CASP-981011	98-10-11	120	3900-5200	100
CASP-981012	98-10-12	120	3900-5200	100
FERO-990721	99 07 21	90	3600-9000	35
FERO-990801	99-08-01	90	3600-9000	40

* Quoted S/N ratios are measured at 6700 Å on the EMMI spectra, and at 5100 Å on the FEROS and CASPEC spectra.

Table 2. Radial velocity observations of CS 22873-139

spectrum	JD 2450000+	V_r		Phase
		primary kms^{-1}	secondary kms^{-1}	
EMMI-971018	739.6	254.8	213.8	0.819
EMMI-971020	741.6	263.1	201.5	0.924
EMMI-990811	1401.7	212.2	259.2	0.381
CASP-981011	1097.6	220.6	258.3	0.511
CASP-981012	1098.6	224.3	253.0	0.566
FERO-990721	1380.7	215.3	256.1	0.277
FERO-990801	1391.7	257.4	212.5	0.851

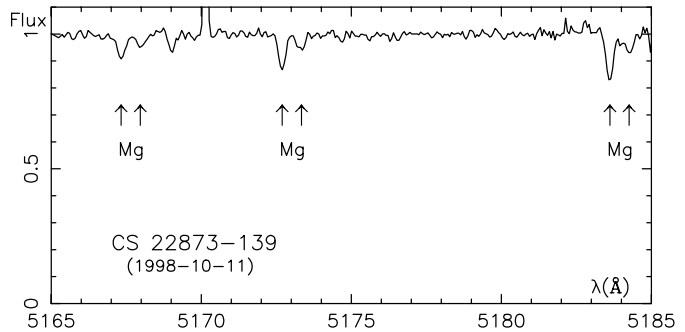
FEROS instrument on the ESO 1.5m telescope was used to obtain lower S/N spectra in order to provide additional (independent) information for the velocity zero point of this star, as our initial inspection of the EMMI data suggested the presence of a possible offset with respect to the values provided by Preston (1994) (see below).

The observing log is given in Table 1. All the spectra have been reduced with a semi-automatic code developed for échelle spectra at Paris-Meudon Observatory (Spite 1990). The code locates the spectral orders by optimal extraction and performs flat fielding and wavelength calibration from the comparison lamp spectrum with a minimum of user intervention. The S/N ratios in Table 1 have been directly measured on the spectra. Preliminary results have been published (Nordström et al. 2000).

3. Radial velocity measurements

In the majority of our spectra the lines of the two components are well separated, and we were able to obtain measurements of the individual radial velocities of the primary (A) and the secondary (B) stars. A sample spectrum is shown in Fig. 1. To obtain an independent check on the radial velocity measurements, two additional spectra were obtained with the new high-resolution spectrograph FEROS (see Kaufer et al. 1999) on the ESO 1.5m telescope at La Silla. These spectra have a lower S/N ratio and have not been used for elemental abundance measurements.

As a result of the very low metallicity of CS 22873-139 rather few lines are measurable on the spectra, thus we estimate

**Fig. 1.** Example of spectrum of CS 22873-139 observed with the CASPEC spectrograph in the region of the Mg I triplet at a phase showing a large shift.**Table 3.** New orbital elements for CS 22873-139 (see text)

Element	This paper	Preston (1994)
P	19.166 ± 0.015	19.165
T (HJD - 2 400 000)	48424.33 ± 0.11	48424.1
e	0.200 ± 0.028	0.26
ω	$44.0^\circ \pm 7.1^\circ$	38°
$V_0(kms^{-1})$	235.26 ± 0.39	231.2
$K_A(kms^{-1})$	23.96 ± 0.54	24.5
$K_B(kms^{-1})$	29.15 ± 1.50	28.0

that the accuracy of the radial velocities lies between 1 and 2 kms^{-1} for the primary component (A), and about 3 kms^{-1} for the secondary (B), the lines of which are extremely faint. The results are given in Table 2. We note that several telluric lines are visible in the EMMI and FEROS spectra, and thus the radial velocities could be corrected for small systematic errors which might be present. In the CASPEC spectra no telluric lines could be used, thus a small systematic error in the radial velocities cannot be excluded.

The better resolution and time coverage provided by the ESO observations allow us to improve the determination of the period and check the other parameters of the binary orbit. Preliminary orbital solutions showed that Preston's velocities for the primary star (A) were, on average, 3 kms^{-1} below ours (and Preston later explained this shift). As the latter were checked with the telluric absorption lines (see above), we added 3 kms^{-1} to Preston's velocities and made a new least-squares solution for the orbital elements of star A, for which Preston's velocities are presumably least affected by blending with lines of the other star. Fixing e and ω , we then solved again for the orbital elements, giving Preston's observations half weight of the ESO data for star A and retaining only the ESO observations for star B, for which Preston's data show large scatter and only marginal resolution of primary and secondary lines.

The result is given in Table 3 and shown in Fig. 2. As will be seen, we find a slightly lower eccentricity and larger ω and K_B than Preston. However, the results depend critically on an apparent systematic shift of 3–4 kms^{-1} in the new CASPEC data (we find a mass ratio $q = M_2/M_1 = 0.92 \pm 0.03$; including the CASPEC data leads to a considerably smaller value). Until

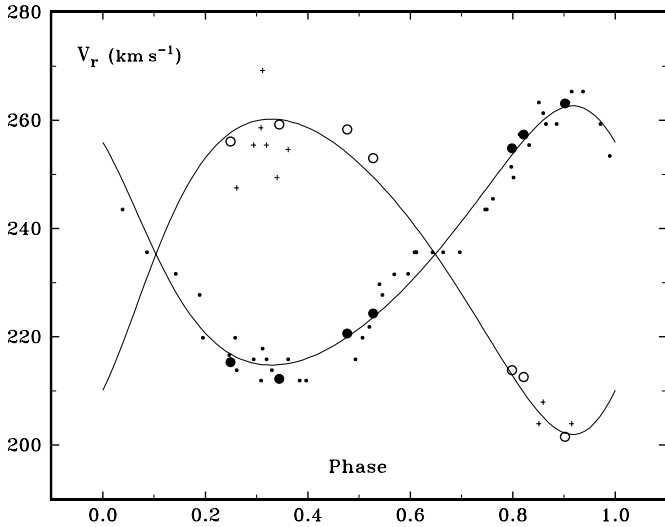


Fig. 2. Spectroscopic orbits of CS 22873-139. Small dots and pluses denote Preston's velocities (corrected by $+3 \text{ km s}^{-1}$ - see text), large dots and circles the new ESO velocities for star A and B, respectively. The two curves have been computed with the orbital elements of Table 3.

more definitive data become available, we shall assume $q = 0.90 \pm 0.02$ in the following.

4. Abundance analysis

4.1. Stellar parameters

The models used in the analysis of the stars have been interpolated in the grid of Edvardsson et al. (1993), computed with an updated version of the MARCS code of Gustafsson et al. (1975) with improved UV line blanketing (OSMARCS models, see also Edvardsson et al. 1993). To compute the parameters of the stars we made the hypothesis that the star is a normal halo star (not very young), and used the isochrone of Vandenberg et al. (2000) computed for 12 Gyr and a metallicity of $[\text{Fe}/\text{H}] = -2.3$.

The derivation, from the composite spectrum, of the atmospheric parameters of the A and B components of CS 22873-139 has been performed by successive iterations. We assumed that the two components have been formed together and thus have the same age, the same metallicity and differ only by their mass. A first approximation of the temperature of the A component is found from the profile of the wings of the H_α line. Then its mass is read on the table of Vandenberg et al. (2000) corresponding to the isochrone, the mass of the B component is computed from $M_B/M_A = 0.90$ and its parameters (temperature, absolute magnitude) are read in Vandenberg's table. The temperatures given by Vandenberg et al. have been shifted by 0.01 in $\log T_{\text{eff}}$ (as needed to fit high parallax subdwarfs following Cayrel et al. 1997). The ratio of the fluxes are then deduced from the difference in magnitude. The obtained parameters are used to compute a second approximation of the composite profile of the hydrogen lines. A fast convergence is obtained (the wings of the H lines are not very sensitive to the parameters of the

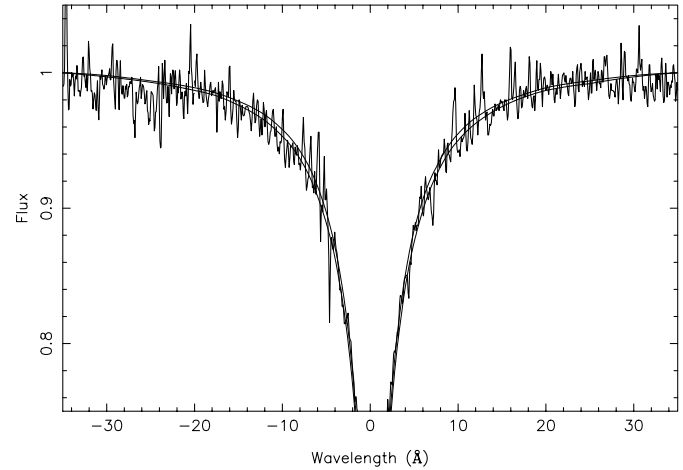


Fig. 3. An example of the H_α profile, computed with two different sets of temperatures 6300-5750 and 6400-5850 and a flux ratio of 0.4 (cf also Table 4) compared to the observed spectrum EMMI-990811.

companion). We find a flux ratio F_B/F_A in the B band equal to 0.40 (to be compared to 0.33 following Preston).

Let us remark that this isochrone is the most metal deficient computed by Vandenberg (it corresponds to the most metal-deficient globular clusters), it has been computed using a He abundance $Y = 0.235$, and an enhancement of the α -elements of 0.3 dex. Since our object turns out to be without the usual enhancement of α -elements in Pop I stars (cf Sect. 5.2), it has to be considered that the isochrone, computed for $[\text{Fe}/\text{H}] = -2.3$ dex, is in fact computed for a higher global metallicity: the isochrone is equivalent (Salaris et al. 1993) to a non-enhanced isochrone with $[\text{Fe}/\text{H}] = -2.3 + 0.25 = -2.05$ dex. Our stars are more metal deficient than this value, but they are far enough from the turn-off for keeping the same flux ratio as the ratio which would be measured on an isochrone computed for a lower metallicity.

In Fig. 3 we present an example of the fit of computed and observed H_α profiles. To determine the observed profile on the échelle spectra, the Gehren method has been used (Gehren 1990). In this method, often used, the continuum is fitted, *not* by an arbitrary polynomial, but by the mean of the observed blaze functions of the preceding and following orders (a method extensively used by the group of Gehren and Fuhrmann, in several papers by the Spite group and in particular Spite et al. 1996). For a good S/N ratio, this method gives, for spectra not crowded with absorption lines, an accuracy better than 0.5%, which corresponds to a random error of about 100 K in the temperature of each component. In the particular (more difficult) case where two different stars contribute to the observed spectrum, an estimation of the temperature error of 200 K for each star seems reasonable. (Of course there still remains the question of the existence of a possible additional systematic error). The position of the two components in the HR diagram is shown in Fig. 4.

The colors of the stars, following Vandenberg et al. (2000), are $B-V = 0.37$ and 0.51 , resulting in $(B-V)_o = 0.41$ for the binary: in disagreement with the bluer color observed by Preston

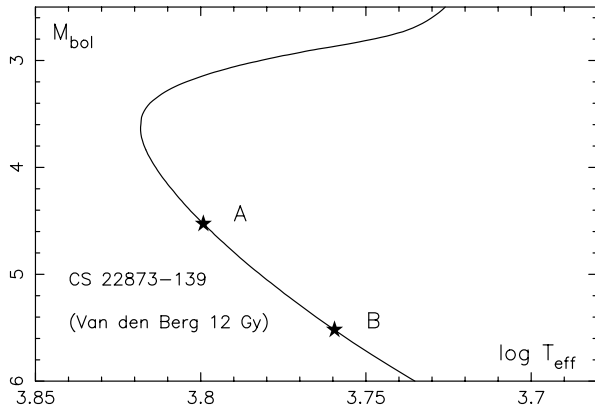


Fig. 4. Position of the two components of CS 22873-139 on the isochrone of Vandenberg et al. 2000, computed for 12 Gyr and $[\text{Fe}/\text{H}] = -2.3$

Table 4. Best atmospheric parameters for the A and B components

Star	T_{eff}	$\log g$	V_t km s^{-1}	normalised flux at 5000 Å
CS 22873-139 A	6300 K	4.2	1.3	1
CS 22873-139 B	5750 K	4.5	1.3	0.40

et al. (1994), leading in Preston’s paper to a higher temperature and a lower age. We discuss this problem in Sect. 4.3: in absence of any definite solution for this discrepancy, we will compute the abundances in both cases: low temperature and age of 12 Gyr, higher temperature and age of 8 Gyr (isochrones of Vandenberg et al. 2000). We begin with the first solution.

4.2. Atomic parameters and results

For iron, the $\log gf$ values are taken from Nave et al. (1994). The $\log gf$ values for Ti II are from Wiese & Fuhr (1975) and those for Na I, Mg I, Ca I, Sc II and Sr II are as adopted by Ryan et al. (1991). The measurements have been made individually on each spectrum.

We found that the best agreement with our observed spectra was obtained with the atmospheric parameters listed in Table 4 (see also Fig. 3). The results of the elemental abundance computations are given in Table 5.

The mean abundances we derive for individual elements are given in Table 6. Fig. 5 shows an example of the best fit in the region of the Mg I 5172.7 Å line. The major error source in $[\text{Fe}/\text{H}]$ is due to the error in T_{eff} . A change in T_{eff} of +200 K corresponds to a change in $[\text{Fe}/\text{H}]$ of typically +0.14 dex. Effects of errors in abundance ratios like $[\text{Mg}/\text{Fe}]$ are negligible.

4.3. Analysis with Preston’s parameters (2nd solution)

We have noted hereabove that the profile of the $\text{H}\alpha$ line leads to temperatures too low for an agreement with the observed colors. Preston has computed that the global color $B - V = 0.37$

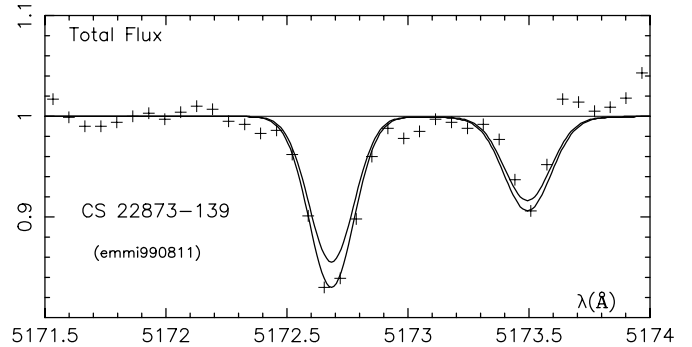


Fig. 5. Fit of the synthetic spectrum to the spectrum observed in August 1999 in the region of the Mg I 5172.7 Å line, for two magnesium abundances $\log \epsilon(\text{Mg}) = 4.1$ and 4.25. The lines of the primary and secondary are well fitted by an intermediate value. The final value (Table 6) 4.17 dex results from the fits of five individual spectra.

would correspond to $(B - V)_0 = 0.30$ for the primary, leading to an age of 8 Gyears. An independent color measurement $(b - y)_o = 0.27$ (Schuster et al. 1996) also provides a hotter global temperature ($T_{\text{eff}} = 6423$ K). The reddening estimation of a binary is probably somewhat uncertain, but the reddening value is in agreement with the modern reddening maps (Schlegel et al. 1998).

We have therefore computed the parameters of the stars which would correspond to bluer colors. Using the table of Vandenberg which corresponds to an isochrone of 8 Gyr, we deduced that the temperature of the primary would be 6760 K and the temperature of the secondary 6160 K. With these parameters we computed also the abundances of the different elements: these abundances are also given in the Table 6.

The metallicities of the stars are a little higher (since the stars are supposed to be hotter) but it is important to remark that the ratios of the different elements like $[\text{Mg}/\text{Fe}]$ do not change significantly.

The discrepancy between the spectroscopic and photometric temperature indicators, remains a problem, and several hypotheses may be imagined. For example, owing to the relatively high value of the c_1 index, it cannot be completely excluded that the primary is a subgiant (or even a red HB star): Schuster et al. (1996) consider such a possibility for a few stars with a high c_1 index (their Sect. 3.1), and Norris et al. (2000) discuss this point for the rather similar binary that they analyze (but their star has a low c_1 index). At first, we noted that the ionisation equilibrium is not as good, in the second solution (hotter temperature) as it is in the first one, but since only one Fe II line can be measured in this very metal poor star, this fact is not a strong argument in favor of the low temperature solution.

Rather than further speculate about more or less different solutions, a check of the spectroscopic temperature should be made first. Unfortunately, the $\text{H}\beta$ line is registered, in our spectra, on the edge of the detector, no accurate measurement can be made, and the most urgent thing to do is to observe again both $\text{H}\alpha$ and $\text{H}\beta$ using a better suited spectrograph (we will do it in the future).

Table 5. Abundances computed for the different lines of elements, using the parameters given in Table 4. In Columns 4 to 8 the logarithmic abundances of the different elements, $\log \epsilon(M)_*$, are given using the convention $\log \epsilon(H)_*=12$. In the last column, the mean value for each line

line	elem	$\log gf$	EMMI-971018	EMMI-971020	EMMI-990811	CASP-981011	CASP-981012	$\log \epsilon(M)_*$
5890.0	Na I	0.112			2.40			2.4
5172.7	Mg I	-0.38	4.12	4.10	4.30	4.12	4.20	4.17
5183.6	Mg I	-0.16	4.10	4.30	4.20	4.15	4.10	4.17
3944.0	Al I	-0.64					≤ 2.3	≤ 2.3
3961.5	Al I	-0.34				2.30	2.30	2.30
4226.7	Ca I	0.24				3.15	3.15	3.15
4045.8	Fe I	0.28				4.20	4.20	4.20
4063.6	Fe I	0.06				4.10	4.05	4.08
4071.7	Fe I	-0.02				4.15	4.10	4.13
4143.9	Fe I	-0.51				4.15	4.15	4.15
4202.0	Fe I	-0.71				4.10	4.10	4.10
4271.8	Fe I	-0.16				4.15	4.05	4.10
4383.6	Fe I	0.20				4.10	4.15	4.13
4404.8	Fe I	-0.14				4.15	4.15	4.15
5169.1	Fe II	-0.97			4.20	4.10	4.00	4.10
4395.0	Ti II	-0.65				2.10	2.05	2.08
4443.8	Ti II	-0.81				2.25	2.10	2.18
4468.5	Ti II	-0.77				2.30	2.15	2.23
4501.3	Ti II	-0.86				2.10	2.10	2.10
4534.0	Ti II	-0.76				2.30	2.25	2.28
4077.7	Sr II	0.15				≤ -1.5	≤ -1.5	≤ -1.5

5. Discussion

5.1. The lithium abundance

In main-sequence turnoff stars the lithium lines are always weak and difficult to measure. All the more so when the spectrum of a component is veiled by the underlying flux of a companion star, as it the case for CS 22873-139. In an effort to increase the signal to noise ratio, we co-added the three EMMI spectra of the star in the lithium region although the distance of the lines of the two components is different. First we co-added the spectra centered on the line of the A component (to measure the lithium line of the A component), and second we co-added the spectra centered on the line of the B component (to measure the lithium line of the B component). In neither of these cases could the lithium line be detected. However, if the models 6300/5750 are adopted the upper limit of the lithium line remains compatible with a lithium abundance $\log \epsilon(\text{Li}) \sim 1.90$ dex (Fig. 6). It happens that this lithium abundance is in agreement with the trend predicted by Ryan et al. (1996), but this agreement would have a real meaning only if our temperature determination was in the same scale as the one used for defining this trend (our temperature is derived from the line fitting). If the models 6760/6160 are adopted, the lithium profile would be even compatible with a lithium abundance up to $\log \epsilon(\text{Li}) \sim 2.3$ dex.

Let us note that Thorburn (1994), finds an equivalent width of 17 mÅ, from the measure of the line (on a spectrum with $S/N = 75$), amplified by enhancement through an estimated dilution factor. The two components are assumed to be near the turnoff, a temperature of 6423 K is estimated (exactly the same as the

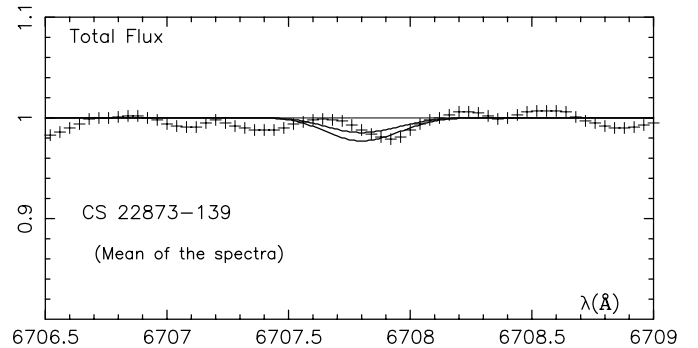


Fig. 6. Fit of the synthetic spectrum of the lithium doublet and of the mean observed spectrum (centered on the A component) in the region of the lithium line, for two lithium abundances $\log \epsilon(\text{Li})=1.9$ and 1.7. The lithium line is not detected, but this remains compatible with a lithium abundance up to $\log \epsilon(\text{Li}) = 1.90 \pm 0.15$ dex with the low temperature solution, and even higher with the high temperature (based on colors).

one provided by Schuster et al. 1996), resulting in a lithium abundance $\log \epsilon(\text{Li}) = 2.28$ dex. Ryan et al. (1996a) adopt a similar temperature, and derive a lithium abundance $\log \epsilon(\text{Li}) = 2.15$ dex.

5.2. Abundance anomalies

In Table 6, two abundance anomalies may be recognized. The most striking is the very low abundance of Sr (Fig. 7). In main-sequence turn-off stars, the strong resonance lines of Sr II at 4077 and 4215 Å usually persist even in very metal-poor stars

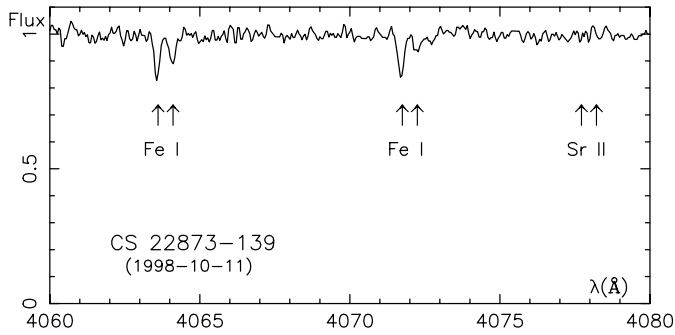


Fig. 7. Example of a spectrum of CS 22873-139 obtained on October 1998 with the CASPEC spectrograph in the region of the Sr II line at 4077.7 Å

Table 6. Abundances of the different elements in the Sun and in CS 22873-139 for the model deduced from the profile of the H α line, and the model deduced from the colors of Preston $[M/H]_P$

element	$\log \epsilon_{\odot}$	$\log \epsilon_*$	$[M/H]$	$[M/H]_P$
FeI	7.50	4.13	-3.37	-3.02
FeII	7.50	4.13	-3.40	-3.33
Na	6.33	2.40	-3.93	-3.58
Mg	7.58	4.17	-3.41	-3.14
Al	6.47	2.30	-4.17	-3.82
Ca	6.36	3.15	-3.36	-2.88
Ti	5.02	2.17	-2.85	-2.78
Sr	2.97	≤ -1.50	≤ -4.47	≤ -4.40

(see Fig. 11 of Ryan et al. 1991). The second anomaly is the low abundance of the α -elements Mg and Ca, (but an overabundance of Ti), which is not the usual behavior in most metal-poor stars.

A few extremely metal-poor stars ($[Fe/H] < -3$) are known with a very low abundance of strontium (Molaro & Bonifacio 1990, Ryan et al. 1991, Norris et al. 1993, Primas et al. 1994, McWilliam et al. 1995a, 1995b and Ryan et al. 1996b). Abundance ratios for a number of elements in these stars are given in Table 7, where we list the stars with $[Sr/Fe] < -1$. The stars CS 22885-096 and CS 22968-014 have been studied by three different authors. The agreement between the different determinations is rather good for CS 22885-096, but for CS 22968-014 the spread of the element-ratios from author to author is large, although the models used are very close. To improve the quality of the abundances we have averaged the three lists of published equivalent widths, and we re-computed the abundances, in a homogeneous manner, directly from the equivalent widths. We adopted $T_{\text{eff}} = 4950$ K, $\log g = 2.0$ and $v_t = 1.9$ km s $^{-1}$ (Primas et al. 1994). This star is a cool giant (4900 K) and thus the equivalent widths of the magnesium lines are about 100 m Å and the magnesium abundance is very sensitive to a small variation of the equivalent widths. On the other hand, the Ti II lines are all weak and a good signal to noise is important to measure weak lines. The result of these computations is given in Table 7.

All the stars known to exhibit a very low strontium abundance are extremely metal-poor. Ryan et al. 1991 remark that

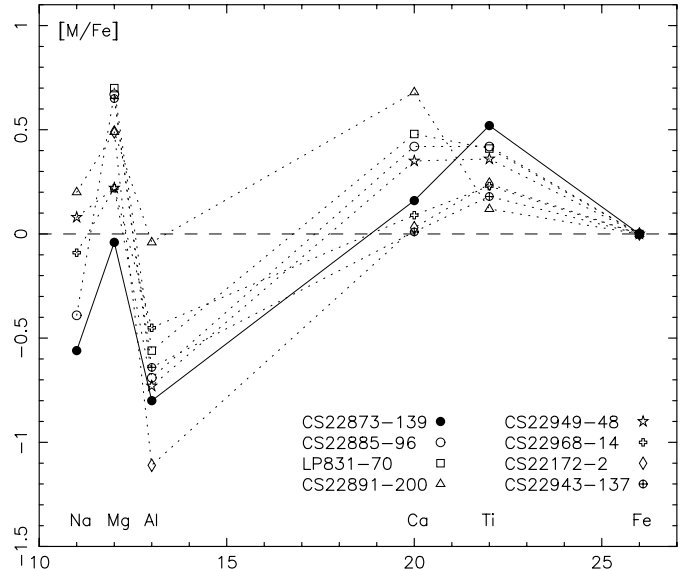


Fig. 8. Abundances of the elements relative to iron in the seven strontium-poor stars and in CS 22873-139 versus the atomic number Z . The elements formed by the α -process are linked by a full (CS 22873-139) or dotted (other Sr-poor stars) line.

their Sr-weak stars are among the most metal-poor stars of their sample and that, as a consequence, a possible explanation of their Sr deficiency is that they have been formed out of material issued from stars initially deprived of iron (and of course of Sr), i.e. from Pop III stars (first generation stars). The first generation of stars, when becoming SN II, would have synthesized iron-peak elements which could be transformed into heavy elements like Sr only in a second generation of (massive) stars. Our binary star, like the seven other Sr-weak stars in Table 7, could thus be a second generation (low-mass) object which did not initially possess any secondary elements, and for which even the amount of primary heavy elements is very small. Also, Cayrel (1996) has noted a global correlation between the abundance of Sr and the metallicity in very metal-poor stars.

If we suppose that CS 22873-139 is a second generation star, we could expect that the material from which it has been formed has been enriched only by SN IIe, and probably, only by a few SN IIe (or even by a single one) and it is important to compare the detailed abundances with those predicted by recent nucleosynthesis computations.

In Fig. 8 we compare the abundances (relative to iron) to the solar abundances, in the seven Sr-poor stars of Table 7 and in CS 22873-139. In the Sr-poor stars, the elements Mg, Ca, and Ti are generally overabundant relative to iron as it is normally observed in the Pop II stars. In CS 22873-139, $[Mg/Fe]$ and $[Ca/Fe]$ are close to zero, while Ti is enhanced. Titanium is not a typical α -process element (contrary to Mg and Ca), and indeed may also be formed by the e -process (e.g. Wallerstein et al. 1997).

The abundance ratios relative to iron in CS 22873-139 are not very different from CS 22968-014, which presents only a

Table 7. Relative abundances of the elements in CS 22873-139 compared to the seven other extremely metal-poor stars with very low strontium abundance ($[\text{Fe}/\text{H}] < -3.0$, $[\text{Sr}/\text{Fe}] < -1$). For CS22885-096 the last line gives the mean value of the abundances computed by the different authors. For CS 22968-014 where the results were rather discordant, the equivalent widths have been averaged and the abundances re-computed in an homogeneous way.

Star	Ref*	[Fe/H]	[Sr/Fe]	[Na/Fe]	[Mg/Fe]	[Al/Fe]	[Ca/Fe]	[Ti/Fe]
CS 22873 – 139	this paper	-3.37	< -1.10	-0.56	-0.04	-0.80	+0.16	+0.52
CS 22885 – 096	MB90	-4.21	< -1.25	-0.67	+0.93	-	+0.35	+0.36
CS 22885 – 096	MPSS95	-3.79	-1.35	-0.11	+0.46	-0.80	+0.58	+0.36
CS 22885 – 096	NPB93	-4.24	-1.17	-	+0.72	-0.47	+0.28	+0.79
CS 22885 – 096	RNB96	-3.60	-1.54	-	+0.57	-0.81	+0.46	+0.16
CS 22885 – 96	Mean value	-3.96	-1.35	-0.39	+0.67	-0.69	+0.42	+0.42
LP 831 – 70	RNB91	-3.40	< -1.1	-	+0.70	-0.56	+0.48	+0.41
CS 22891 – 200	MPSS95	-3.49	-1.33	+0.20	+0.49	-0.04	+0.68	+0.12
CS 22949 – 48	MPSS95	-3.17	-1.48	+0.08	+0.22	-0.73	+0.35	+0.36
CS 22968 – 014	NPB93	-3.77	-1.54	-	+0.39	-0.78	+0.08	+0.52
CS 22968 – 014	PMC94	-3.45	-1.52	-0.20	+0.02	-0.87	+0.01	+0.59
CS 22968 – 014	MPSS95	-3.41	-1.80	-0.35	-0.06	-0.73	+0.10	+0.15
CS 22968 – 014	RNB96	-3.43	-1.81	-	+0.64	-0.90	+0.22	+0.27
CS 22968 – 014	this paper	-3.30	-1.54	-0.09	+0.22	-0.45	+0.09	+0.23
CS 22172 – 002	RNB96	-3.57	-1.36	-	+0.49	-1.11	+0.03	+0.24
CS 22943 – 137	RNB96	-3.22	< -1.43	-	+0.65	-0.64	+0.01	+0.18

* MB90 Molaro & Bonifacio 1990, RNB91 Ryan et al. 1991, NPB93 Norris et al. 1993, RNB96 Ryan et al. 1996b, PMC94 Primas et al. 1994, MPSS95 McWilliam et al. 1995.

small overabundance of Mg and Ca relative to iron, but the ratio $[\text{Ti}/\text{Fe}]$ is (probably) significantly different.

Some kind of similarity in the abundance pattern seems to appear in Fig. 8, blurred by variations of Fe abundance, and it was hoped that, by cancelling these variations of Fe, the similarity would show up: in Fig. 9, the ratios were normalized to Mg (rather than to Fe), but the spread of abundances for Ca is not reduced, and the Ti spread is worse. Adding or not adding some Fe, does not solve the lack of similarity.

An explanation of a low ratio α -elements/Fe could be the addition of Fe by a SN Ia but the very low iron abundance in the stars considered here is against this hypothesis, as well as the fact that the spread in the abundances Mg/Fe, Ca/Fe and Ti/Fe does not show the signature of a simple iron addition, as noted before.

It is also interesting to compare the abundances of CS 22873-139 to the abundances of CS 22876-32 another extremely metal-poor binary star recently studied by Norris et al. (2000) with $[\text{Fe}/\text{H}] = -3.7$. In this star the $[\text{Sr}/\text{Fe}]$ is < -0.65 and thus it does not appear in Table 7 (stars with $[\text{Fe}/\text{H}] < -3.0$ and $[\text{Sr}/\text{Fe}] < -1$), but the strontium abundance is certainly rather low in this star. However CS 22876-32 unlike CS 22873-139, is magnesium rich: $[\text{Mg}/\text{Fe}] = +0.50$. It is only moderately Ca and Ti rich: $[\text{Ca}/\text{Fe}] = +0.13$ and $[\text{Ti}/\text{Fe}] = +0.11$.

Two common proper motion stars (HD 134439 - HD 134440) show abundance anomalies similar to those of our binary, they have retrograde orbits (which are sometimes interpreted as a sign of accretion and particular nucleosynthesis

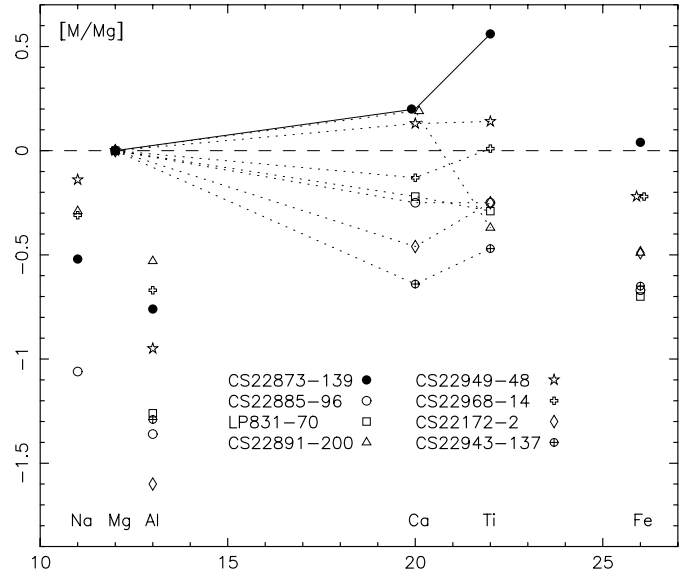


Fig. 9. Abundances of the elements relative to magnesium versus Z in the seven already known very Sr-poor stars and in CS 22873-139. The elements formed by the α -process are linked by a full (CS 22873-139) or dotted (other Sr-poor stars) line.

history). The deficiency of HD 134439 is moderate: only $[\text{Fe}/\text{H}] \approx -1.7$ (King 1997, Ryan et al. 1991) but $[\text{Mg}/\text{Fe}] = -0.02$, $[\text{Ca}/\text{Fe}] = +0.19$ and $[\text{Ti}/\text{Fe}] = +0.36$. Strontium is also rather weak in HD 134439, $[\text{Sr}/\text{Fe}] = -0.77$. The abundance pattern

of CS 22873-139 is therefore strikingly similar to the pattern found in HD 134439.

It has to be noted that all the very Sr-poor stars have to be formed before the addition of the ejecta of massive AGB (which form and eject s-process elements) and therefore relatively rapidly after the explosion of the SN IIe, owing to the relatively short time scale of the evolution of the AGB, and of the mixing of the AGB products by their wind.

Since our star does not show the usual enhancement of α -elements (found in the observations of Pop II stars and in the predictions of SN II yields averaged over the IMF), we can try to compare the abundance pattern to the predictions of nucleosynthesis in individual SN II. For example, recent computations by Umeda et al. (2000) predict no overabundance of Mg and Ca relative to Fe in the ejecta of a $20 M_{\odot}$ SN II of zero metallicity. The models of Umeda et al. predict for such SN IIe, large deficiencies of Na and Al (odd-even effect) and these deficiencies are found in our star (and in most of the other Sr-poor stars, but not all). The predicted odd-even effect is however about twice as large as observed in our star, although a NLTE analysis would provide a lower Na abundance, following Baumüller et al. (1998). Moreover, Ti is predicted to be deficient (and observed abundant). Umeda et al. consider (cf. their Sect. 8.3) that the yield of hypernovae could possibly explain the relatively high abundance of Ti.

Perhaps the ratios of the abundances to Fe are not essential, since the mass-cut parameter is rather uncertain, the relative abundances of the elements Mg, Ca and Ti (and the deficiencies of Na and Al) are maybe more informative.

The SN II models predict, for other masses, an enhancement of the α -elements: for example the $25 M_{\odot}$ model of Umeda et al. (2000) predicts Ca more enhanced than Mg (Al and Na remaining deficient): this could fit for example, the star CS 22885-96.

Also, models of Nomoto et al. (1997) for SN IIe more massive than $18 M_{\odot}$, predict an enhancement of Mg/Fe and even, for masses of $40 M_{\odot}$, an enhancement of both Mg/Fe and Ca/Fe, but strong deficiencies of Na and Al are not predicted: these models could fit stars such as CS 22891-200. On the contrary, most of the Sr-poor stars do not fit the abundances shown by the global product (averaged over the IMF) of the SN IIe of various masses (Fig. 8 of Nomoto et al. 1997).

Let us recall that one explanation proposed in the literature for stars with a low α -elements/Fe ratio, is a late star formation, from primordial matter polluted by already evolved matter, i. e. matter which has already reached solar abundance ratios. But this explanation does not fit well the Sr-poor stars which are presumably second generation stars.

Another explanation is that the stars are from a region of low star formation rate (or of infrequent bursts) so that solar ratios (due to the addition of the ejecta of SN Ia) can be reached at low metallicity. Again this explanation does not fit well the very iron-poor and Sr-poor stars (as noted above, the stars have to be formed quickly after the explosion of the SN II, *before* a large formation of s-elements by the AGB).

Finally, it appears that the the most likely explanation could be that the very metal deficient and Sr-poor stars seem to reflect

the products of few (or even of a single) zero-metal SN II, or hypernovae, and do not follow the mean abundances obtained by the integration of the products of the SN IIe, averaged over the standard IMF.

6. Conclusion

CS 22873-139 is a high velocity, very metal-deficient double-lined binary. Five high resolution spectra at five different phases have been analyzed individually. The wings of the hydrogen lines indicate a rather low temperature, the colors seem to suggest a significantly hotter temperature, which would imply a smaller age. This problem has to be solved by more detailed observations. The abundances of the elements have been computed with the temperature indicated by the wings of the Hydrogen lines, but they have also been computed for the higher temperature indicated by the $B-V$ color: the *ratios* of metal abundances are not significantly changed.

The large deficiency together with the lack of detection of Sr suggest that this star, born in a primitive phase of evolution, is perhaps a second generation star: the abundances in this star are therefore interesting.

The lithium line (veiled by the companion) is not measurable, but the upper limit of the lithium abundance may reach $\log\epsilon(\text{Li}) \sim 1.9$ dex if the temperature is found from the hydrogen lines, and 2.3 dex if we rely on the photometry.

This very deficient star does not display the enhancement of the α -process elements, generally observed in the Pop II stars. The usual interpretations proposed in the literature for this non-enhancement of the α -elements do not seem to be adequate for stars which are both very deficient and very Sr-poor.

A possibility is a direct comparison of the abundance pattern with the predictions of the yields of individual models of zero-metallicity SN II. For some given masses of SN IIe, the models of Umeda et al. (2000) do not predict a significant enhancement of the α -process elements. Such models could fit the stars which do not show an enhancement of α -elements. In particular, a single SN II of $20 M_{\odot}$ could fit our star rather well, according to the model of Umeda et al., in spite of a discrepancy for Ti. Let us note that the definitive model atmosphere of the star could turn out to have a smaller gravity, which would imply a slightly lower abundance of Ti. As another possibility, Umeda et al. consider that the progenitor(s) of CS 22873-139 is(are) one(several) hypernova(e). The yields predicted for the SN IIe show significant variations from mass to mass and of different masses models could fit other Sr-poor stars, which show different abundance patterns.

It could then be that the abundances of each very deficient *and* very Sr-poor star reflect the products of a few (or even a single) SN II. Further analyses of extremely metal-deficient stars, are promising and should be rewarding.

Acknowledgements. We thank the referee, George Preston, for kindly confirming the small zero-point shift that we found in the radial velocities published in his 1994 paper, and for helpful remarks which have enabled to improve the paper. We are indebted to Don Vandenberg

for providing isochrones in advance of publication, and John Norris for providing results on CS 22876-32 in advance of publication. The Carlsberg Foundation is gratefully acknowledged for financial support to BN. This work has made use of the CDS, operated by the CNRS.

References

- Baumüller D., Butler K., Gehren T., 1998, *A&A* 338, 637
 Beers T.C., Preston G.W., Shectman S.A., 1985, *AJ* 90, 2089
 Beers T.C., Preston G.W., Shectman S.A., 1992, *AJ* 103, 1987
 Cayrel R., 1996, *A&AR* 7, 217
 Cayrel R., Lebreton Y., Perrin M.-N., Turon C., 1997, *ESA Symposium Hipparcos-Venice 97*, Venice, Italy, ESA SP-402, p. 219
 Edvardsson B., Andersen J., Gustafsson B., et al., 1993, *A&A* 275, 101
 Gehren T., 1990, In: Baade D., Grosbøl P.J. (eds.) *2nd ESO/ST-ECF Data Analysis workshop, ESO Conference and Workshop Proceedings No. 34*, Garching, p. 103
 Gustafsson B., Bell R.A., Eriksson K., Nordlund A., 1975, *A&A* 42, 407
 Kaufer A., Stahl O., Tubbesing S., et al., 1999, *The Messenger*, ESO 95, 8
 King J.R., 1997, *AJ* 113, 2302
 McWilliam A., Preston G., Sneden C., Shectman S., 1995a, *AJ* 109, 2736
 McWilliam A., Preston G., Sneden C., Searle L., 1995b, *AJ* 109, 2757
 Molaro P., Bonifacio P., 1990, *A&A* 236, L5
 Nave G., Johansson S., Learner R.C.M., Thorne P., Brault J.W., 1994, *ApJS* 94, 221
 Nomoto K., Hashimoto M., Tsujimoto T., et al., 1997, *Nuclear Physics A* 616, 79
 Nordström B., Depagne E., Spite M., et al. 2000, In: Weiss A., Abel T.G., Hill V. (eds.) *The First Stars. Second MPA/ESO workshop*, Springer, Heidelberg, p. 64
 Norris J.E., Beers T.C., Ryan S.G. 2000, submitted
 Norris J.E., Peterson R.C., Beers T.C., 1993, *ApJ* 415, 797
 Preston G., 1994, *AJ* 108, 2267
 Preston G., Beers T.C., Shectman S.A., 1994, *AJ* 108, 538
 Primas F., Molaro P., Castelli F., 1994, *A&A* 290, 885
 Ryan S.G., Norris J.E., Bessell M.S., 1991, *AJ* 102, 303
 Ryan S.G., Beers T.C., Deliyannis C.T., Thorburn J.A., 1996a, *ApJ* 458, 543
 Ryan S.G., Norris J.E., Beers T.C., 1996b, *ApJ* 471, 254
 Ryan S.G., Norris J.E., Beers T.C., 1999, *ApJ* 523, 654
 Salaris M., Chieffi A., Straniero O., 1993, *ApJ* 414, 580
 Schlegel D.J., Finkbeiner D.P., Davis M., 1998, *ApJ* 500, 525
 Schuster W.J., Nissen P.E., Parrao L., Beers T.C., Overgaard L.P., 1996, *A&AS* 117, 317
 Spite M., 1990, In: Baade D., Grosbøl P.J. (eds.) *2nd ESO/ST-ECF Data Analysis workshop, ESO Conference and Workshop Proceedings No. 34*, Garching, p. 125
 Spite M., François P., Nissen P.E., Spite F., 1996, *A&A* 30, 172
 Thorburn J.A., 1994, *ApJ* 421, 318
 Umeda H., Nomoto K., Nakamura T., 2000, In: Weiss A., Abel T.G., Hill V. (eds.) *The First Stars. Second MPA/ESO workshop*, Springer, Heidelberg, p. 150
 Vandenberg D.A., Swenson F.J., Rogers F.J., Iglesias C.A., Alexander D.R., 2000, *ApJ* 532, 430
 Wiese W.L., Fuhr J.R., 1975, *J. Phys. Chem. Ref. Data* 4, 263
 Wallerstein G., Iben I. Jr, Parker P., et al., 1997, *Rev. of Mod. Phys.* 69, 995